[5] D. Orin and W. Schrader, "Efficient computation of the Jacobian for robot manipulators," *Int. J. Robotics Research*, vol. 3, no. 4, 1984.

[6] B. Paden and S. S. Sastry, "Optimal kinematic design of 6R manipulators," *Int. J. Robotics Research*, vol. 7, no. 2, 1988.

[7] B. Paden, "Lie groups of spatial kinematics," private communication, 1992.

[8] F. Park and D. Pack, "Motion control using the product-of-exponentials kinematic equations," in *Proc. IEEE Conf. Robotics & Automation*, Sacramento, 1991.

[9] F. Park, "The optimal kinematic design of mechanisms," Ph.D. dissertation, Harvard Univ., 1991.

[10] R. P. Paul, *Robot Manipulators: Mathematics, Programming and Control.* Cambridge: MIT Press, 1982.

[11] F. Salam and C. Yoon, "On the computational aspect of the matrix exponentials and their use in robot kinematics," *IEEE Trans. Automat. Contr.*, vol. 3, no. 4, 1986.

Force/Position Regulation of Compliant Robot Manipulators

Stefano Chiaverini, Bruno Siciliano, and Luigi Villani

***Abstract*— Stable force/position regulation of robot manipulators in contact with an elastically compliant surface is discussed in this work. The controller consists of a PD action on the position loop, a PI action on the force loop, together with gravity compensation and desired contact force feedforward. Asymptotic stability of the system in the neighborhood of the equilibrium state is proven via the classical Lyapunov method with LaSalle invariant set theorem. A modification of the Lyapunov function leads to deriving an exponential stability result. Numerical case studies are developed for an industrial manipulator.**

I. Introduction

For typical robotic tasks that require interaction with the environment, contact forces must properly be handled by the robot controller [1]. In such cases, a pure motion controller usually gives poor performance and can even cause instability.

If force sensor information is not available for control purposes, one can assign a suitable dynamic behavior between position and force variables at the contact (e.g., impedance control) [2], [3]. On the other hand, several schemes can be devised which attempt to control both end-effector position and contact force by embedding force measurements in the controller. Hybrid control is perhaps the most widely adopted strategy to force/position control of robot manipulators [4]–[7]. The basic idea is the possibility to choose whether to control position or force along each task space direction through the use of proper selection matrices. Stability of hybrid control was addressed in [8]. The problem of force/position control with force sensory feedback was also treated in [9], [10] for the general case of constrained motion tasks.

A conceptually different approach to force/position control of robot manipulators is the parallel control strategy [11]. As opposed to the hybrid control strategy, both force and position variables are used along the same task space direction without any selection mechanism.

Manuscript received March 10, 1992; revised November 27, 1992 and March 19, 1993. This work was supported by Consiglio Nazionale delle Ricerche under contract 93.00905.PF67.

The authors are with Dipartimento di Informatica e Sistemistica, Università degli Studi di Napoli Federico II, Via Claudio 21, 80125 Napoli, Italy.

IEEE Log Number 9216418.

The effectiveness of the scheme is ensured by the dominance of the force control loop over the position control loop along the constrained task directions where interaction occurs. This makes the scheme suitable to manage contacts with unstructured environment and unplanned collisions, which are known to represent a drawback for hybrid controllers. Extensive description of the parallel approach and performance analysis of a control scheme with full dynamic compensation in the case of contact with an elastically compliant frictionless surface can be found in [12], [13].

In view of real-time implementation, a new parallel control scheme was recently proposed which is based on simple position PD control+ gravity compensation + desired force feedforward + force PI control [14]. A preliminary analysis, inspired by the work in [15], showed asymptotic stability of the system around an equilibrium state. In detail, for given force and position set points, the force error is driven to zero at the expense of a position error at steady state. The proof in [14], however, leads to restrictive conditions on the feedback gains.

This work presents an improved proof of local asymptotic stability based on the Lyapunov direct method with use of LaSalle invariant set theorem [16]. A different Lyapunov function is chosen which results in relaxed conditions on the feedback gains; in particular, the position proportional gain does not directly affect stability of the contact.

The Lyapunov function is further modified to prove local exponential stability of the scheme yielding a new set of conditions to be satisfied for the feedback gains.

The proposed control scheme is tested in simulation on the industrial robot COMAU SMART 6.10R; only the first three joints are considered. The numerical case study confirms the results anticipated in theory.

II. Modeling

The class of robot manipulators considered in this work is that of open kinematic chains of rigid links connected by actuated joints. If the manipulator interacts with the environment, it is convenient to describe its dynamics in an m-dimensional operational space [5] that is the space where manipulation tasks are naturally specified. The equations of motion can be written in the form

$$\boldsymbol{B}(\boldsymbol{x})\ddot{\boldsymbol{x}} + \boldsymbol{C}(\boldsymbol{x}, \dot{\boldsymbol{x}})\dot{\boldsymbol{x}} + \boldsymbol{g}(\boldsymbol{x}) = \boldsymbol{u} - \boldsymbol{f} \tag{1}$$

where $\boldsymbol{x}$ is the $(m \times 1)$ vector of operational variables (usually end-effector location), $\boldsymbol{B}$ is the $(m \times m)$ symmetric and positive definite inertia matrix, $\boldsymbol{C}\dot{\boldsymbol{x}}$ is the $(m \times 1)$ vector of Coriolis and centrifugal generalized forces, $\boldsymbol{g}$ is the $(m \times 1)$ vector of gravitational generalized forces, $\boldsymbol{u}$ is the $(m \times 1)$ vector of driving generalized forces, and $\boldsymbol{f}$ is the $(m \times 1)$ vector of contact generalizes forces exerted by the manipulator on the environment; all operational space quantities are expressed in a common reference frame.

Notice that the model (1) describes an ideal robot system where the effects of joint friction, backlash and elasticity, actuator dynamics, etc. are neglected. This is a common assumption which is reasonable in a suitable operational range.

The $(n \times 1)$ vector $\boldsymbol{\tau}$ of joint actuating generalized forces is computed as

$$\boldsymbol{\tau} = \boldsymbol{J}^T\boldsymbol{u}, \tag{2}$$

where $\boldsymbol{J}$ is the $(m \times n)$ manipulator Jacobian matrix.

When m is equal to the number of joints n and the manipulator moves in a singularity-free region of the workspace, the vector of operational variables constitutes a set of Lagrangian generalized coordinates and $\boldsymbol{B}$ assumes the meaning of a true inertia matrix. Instead, in the case of kinematically redundant manipulators ($m < n$), $\boldsymbol{B}$ is only a pseudo inertia matrix [5].

For the purpose of the present work, the attention is restricted to the case of nonredundant, nonsingular manipulators with $m = n = 3$, i.e., only translational motion and force components are considered. Then, $\boldsymbol{x}$ denotes the end-effector position.

Accurate modeling of the contact between the manipulator and the environment is usually difficult to obtain in analytic form, due to complexity of the physical phenomena involved during the interaction. It is then reasonable to resort to a simple but significant model, relying on the robustness of the control system to absorb the effects of inaccurate modeling. Following these guidelines, the case of an environment constituted by a rigid, frictionless and elastically compliant plane is analyzed. The choice of a planar surface is motivated by noticing that it is locally a good approximation to surfaces of regular curvature. The rigidity of the contact plane allows the neglect of the effects of local deformation at the contact. The total elasticity, due to end-effector force sensor and environment, is accounted through the compliance of the plane. Friction effects are neglected within the operational range of interest.

With the above assumptions, the model of the contact force considered takes on the simple form

$$\boldsymbol{f} = \boldsymbol{K}(\boldsymbol{x} - \boldsymbol{x}_0), \tag{3}$$

where $\boldsymbol{x}$ is the position of the contact point, $\boldsymbol{x}_0$ is a point of the plane at rest, and $\boldsymbol{K}$ is the (3×3) constant symmetric stiffness matrix [17] that establishes a linear mapping between $(\boldsymbol{x} - \boldsymbol{x}_0)$ and $\boldsymbol{f}$; notice that (3) holds only when the manipulator is in contact with the environment and all quantities are expressed in the common reference frame. According to [14], the matrix $\boldsymbol{K}$ can be expressed as

$$\boldsymbol{K} = k\, \boldsymbol{n}\boldsymbol{n}^T \tag{4}$$

where $k > 0$ is the stiffness coefficient acting along the unit vector $\boldsymbol{n}$ orthogonal to the contact plane.

III. Force/Position Regulation

A typical task for a robot manipulator in contact with the environment can be prescribed in terms of a position set point $\boldsymbol{x}_d$ and a force set point $\boldsymbol{f}_d$. It can be recognized that, in general, simultaneous achievement of both set points is not guaranteed.

A viable strategy is to adopt the parallel control approach [11]; this is especially effective in the case of inaccurate contact modeling. The key feature is to have a force control loop working in parallel to a position control loop along each task space direction. The logical conflict between the two loops is managed by imposing dominance of the force control action over the position one. The potential offered by this technique compared to conventional controllers also using force feedback sensory information is extensively discussed in [12], [13].

A force/position parallel controller for the system (1) was proposed in [14], based on position PD control + gravity compensation + desired force feedforward + force PI control, i.e.,

$$\boldsymbol{u} = k_P\, \Delta\boldsymbol{x} - k_D \dot{\boldsymbol{x}} + \boldsymbol{g}(\boldsymbol{x}) + \boldsymbol{f}_d + k_F\, \Delta\boldsymbol{f} + k_I \int_0^t \Delta\boldsymbol{f}\, d\sigma, \tag{5}$$

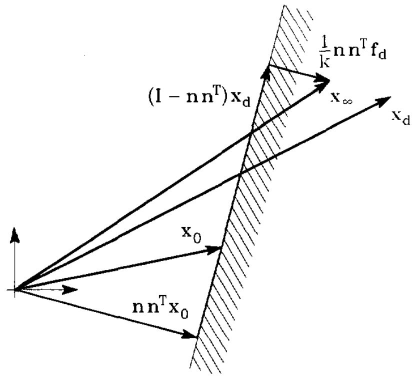

Fig. 1. Construction of the equilibrium point in a two-dimensional case.

where $\Delta\boldsymbol{x} = \boldsymbol{x}_d - \boldsymbol{x}$ is the position error, $\Delta\boldsymbol{f} = \boldsymbol{f}_d - \boldsymbol{f}$ is the force error, and k_P, k_D, k_F, $k_I > 0$ are suitable feedback gains.

It is important to remark that no exact knowledge of the stiffness matrix $\boldsymbol{K}$ is required by the control (5). Notice also that, differently from most force/position control schemes, including the original parallel controller [11], no full dynamic model compensation is required.

The elastic contact model (3) reveals that a null force error can be obtained only if $\boldsymbol{f}_d \in \mathcal{R}(\boldsymbol{K})$. If no information about the geometry of the environment is available, i.e., $\boldsymbol{n}$ is unknown, the null vector can be assigned to $\boldsymbol{f}_d$ that is anyhow in the range space of any matrix $\boldsymbol{K}$. Thus, in the remainder, it is assumed that $\boldsymbol{f}_d \in \mathcal{R}(\boldsymbol{K})$. Analogously, it can be recognized that null position errors can be obtained only on the contact plane, while the component of $\boldsymbol{x}$ along $\boldsymbol{n}$ has to accommodate the force requirement specified by $\boldsymbol{f}_d$; thus, $\boldsymbol{x}_d$ can be freely reached only in $\mathcal{N}(\boldsymbol{K})$, i.e., along the unconstrained directions of the operational space.

As a further assumption, it is supposed that the contact between the manipulator and the environment is not lost after the impact.

As demonstrated in [14], an equilibrium $\{\boldsymbol{x}_\infty, \boldsymbol{f}_\infty\}$ for the system (1) under the control (5) is

$$\boldsymbol{x}_\infty = \frac{1}{k}\boldsymbol{n}\boldsymbol{n}^T(\boldsymbol{f}_d + k\boldsymbol{x}_0) + (\boldsymbol{I} - \boldsymbol{n}\boldsymbol{n}^T)\boldsymbol{x}_d \tag{6}$$

$$\boldsymbol{f}_\infty = k\, \boldsymbol{n}\boldsymbol{n}^T(\boldsymbol{x}_\infty - \boldsymbol{x}_0) = \boldsymbol{f}_d. \tag{7}$$

This is consistent with the above considerations about specification of position and force set points. An example of construction of the equilibrium point in a two-dimensional case is illustrated in Fig. 1.

If the desired force set point $\boldsymbol{f}_d$ is not aligned with $\boldsymbol{n}$, an equilibrium trajectory rather than an equilibrium point is obtained. The expected effect is a drift of the end-effector along the unconstrained directions of the operational space.

IV. Stability

To study stability of the system (1), (3), (5) around $\{\boldsymbol{x}_\infty, \boldsymbol{f}_\infty\}$, define

$$\boldsymbol{e} = \boldsymbol{x}_\infty - \boldsymbol{x} \tag{8}$$

which, by virtue of (3), (6), can be also written as

$$\boldsymbol{e} = (\boldsymbol{I} - \boldsymbol{n}\boldsymbol{n}^T)\,\Delta\boldsymbol{x} + \frac{1}{k}\boldsymbol{n}\boldsymbol{n}^T\,\Delta\boldsymbol{f} = \Delta\boldsymbol{x} + \frac{1}{k_P}\boldsymbol{d} \tag{9}$$

where

$$d = \frac{k_P}{k} \boldsymbol{n}\boldsymbol{n}^T (\boldsymbol{f}_d + k(\boldsymbol{x}_0 - \boldsymbol{x}_d)) \tag{10}$$

is a constant vector taking into account the effects of the environment contact force and the desired force set point.

It should be remarked that the adoption of the model (3) with a constant $\boldsymbol{n}$ is appropriate for the following stability analysis of the system in the neighborhood of the contact equilibrium point for a compliant surface of regular curvature.

For later use, notice that

$$\boldsymbol{n}^T \boldsymbol{e} = \frac{1}{k} \boldsymbol{n}^T \Delta \boldsymbol{f}. \tag{11}$$

From (8) it is

$$\dot{\boldsymbol{e}} = -\dot{\boldsymbol{x}}. \tag{12}$$

Further, define

$$s = \frac{1}{k} \boldsymbol{n}^T \left(\int_0^t \Delta \boldsymbol{f} \, d\sigma - \frac{1}{k_I} \boldsymbol{d} \right). \tag{13}$$

Differentiating (13) with respect to time and taking into account (11) yields

$$\dot{s} = \boldsymbol{n}^T \boldsymbol{e}. \tag{14}$$

At this point, consider the (7×1) augmented state vector

$$z = (\dot{\boldsymbol{x}}^T \quad \boldsymbol{e}^T \quad s)^T. \tag{15}$$

The augmented system described by (1), (12), (14) under the control (5) can be written in the standard compact homogeneous form:

$$\dot{z} = \boldsymbol{F} z \tag{16}$$

where

$$\boldsymbol{F} = \begin{pmatrix} -\boldsymbol{B}^{-1}(\boldsymbol{C} + k_D \boldsymbol{I}) & \boldsymbol{B}^{-1}(k_P \boldsymbol{I} + k'_F k \, \boldsymbol{n}\boldsymbol{n}^T) & k_I k \boldsymbol{B}^{-1} \boldsymbol{n} \\ -\boldsymbol{I} & \boldsymbol{O} & 0 \\ \boldsymbol{0}^T & \boldsymbol{n}^T & 0 \end{pmatrix} \tag{17}$$

with $k'_F = 1 + k_F$; $\boldsymbol{O}$ denotes the (3×3) null matrix and $\boldsymbol{0}$ the (3×1) null vector. Notice that some handy reductions, using the structural properties of $\boldsymbol{K}$ in (4) and the definition of s in (13), have been performed to derive (17).

The following result can be stated:

Theorem 1: There exists a choice of feedback gains k_P, k_D, k_F, k_I that makes the origin of the state space for the system (16), (17) locally asymptotically stable. □

Proof: Consider the Lyapunov function candidate

$$V = \frac{1}{2} z^T \boldsymbol{P} z \tag{18}$$

where

$$\boldsymbol{P} = \begin{pmatrix} \boldsymbol{B} & -\rho \boldsymbol{B} & \boldsymbol{0} \\ -\rho \boldsymbol{B} & (k_P + \rho k_D)\boldsymbol{I} + k'_F k \, \boldsymbol{n}\boldsymbol{n}^T & k_I k \, \boldsymbol{n} \\ \boldsymbol{0}^T & k_I k \, \boldsymbol{n}^T & \rho k_I k \end{pmatrix} \tag{19}$$

with $\rho > 0$. Computing the time derivative of V along the trajectories of the system (16), (17) gives

$$\dot{V} = -\dot{\boldsymbol{x}}^T (k_D \boldsymbol{I} - \rho \boldsymbol{B})\dot{\boldsymbol{x}} - \rho \boldsymbol{e}^T \boldsymbol{C}^T \dot{\boldsymbol{x}} - \boldsymbol{e}^T (\rho k_P \boldsymbol{I} + (\rho k'_F - k_I) k \, \boldsymbol{n}\boldsymbol{n}^T) \boldsymbol{e} \tag{20}$$

in which the skew-symmetry of the matrix $\dot{\boldsymbol{B}} - 2\boldsymbol{C}$ [18]–[20] has been conveniently exploited.

Consider the region of the state space

$$Z = \{z \colon \|\boldsymbol{e}\| < \Phi\}. \tag{21}$$

The term $-\rho \boldsymbol{e}^T \boldsymbol{C}^T \dot{\boldsymbol{x}}$ in(20) can be upper bounded in the region (21) as

$$-\rho \boldsymbol{e}^T \boldsymbol{C}^T \dot{\boldsymbol{x}} \le \rho \Phi k_C \|\dot{\boldsymbol{x}}\|^2 \tag{22}$$

where k_C is a positive constant such that $\|\boldsymbol{C}\| \le k_C \|\dot{\boldsymbol{x}}\|$ [21].

In view of (14), (22), the function (20) can be upper bounded as

$$\dot{V} \le -(k_D - \rho\lambda_M - \rho\Phi k_C)\|\dot{\boldsymbol{x}}\|^2 - \rho k_P \|\boldsymbol{e}\|^2 - k(\rho k'_F - k_I)\dot{s}^2 \tag{23}$$

where λ_M is the maximum eigenvalue of $\boldsymbol{B}$ which is bounded in the case of all revolute joints [22].

On the other hand, the function candidate (18), (19), in view of (14), can be written as

$$V = \frac{1}{2}\dot{\boldsymbol{x}}^T \boldsymbol{B}\dot{\boldsymbol{x}} - \rho \dot{\boldsymbol{x}}^T \boldsymbol{B}\boldsymbol{e} + \frac{1}{2}(k_P + \rho k_D)\boldsymbol{e}^T\boldsymbol{e} + \frac{1}{2}k'_F k \dot{s}^2 + k_I k s \dot{s} + \frac{\rho}{2} k_I k s^2 \tag{24}$$

which can be lower bounded as

$$V \ge \frac{1}{2}(\dot{\boldsymbol{x}}^T \boldsymbol{B} \quad \boldsymbol{e}^T) \begin{pmatrix} (1/\lambda_M)\boldsymbol{I} & -\rho \boldsymbol{I} \\ -\rho \boldsymbol{I} & (k_P + \rho k_D)\boldsymbol{I} \end{pmatrix} \begin{pmatrix} \boldsymbol{B}\dot{\boldsymbol{x}} \\ \boldsymbol{e} \end{pmatrix} + \frac{k}{2}(\dot{s} \quad s) \begin{pmatrix} k'_F & k_I \\ k_I & \rho k_I \end{pmatrix} \begin{pmatrix} \dot{s} \\ s \end{pmatrix}. \tag{25}$$

Equations (23), (25) reveal that there exists a choice of k_P, k_D, k_F, k_I, and ρ that makes V positive definite and $\dot{V}$ negative semidefinite in Z. In fact, (25) gives

$$k_P + \rho k_D > \rho^2 \lambda_M \tag{26}$$

$$\rho(1 + k_F) > k_I \tag{27}$$

while (23) gives

$$k_D > \rho(\lambda_M + \Phi k_C) \tag{28}$$

plus (27) again. Observing that condition (28) implies (26), it can be concluded that only conditions (27), (28) must be satisfied.

Since $\dot{V}$ is negative semidefinite, the inequality $\dot{V} \le 0$ must be further analyzed to prove asymptotic stability. In particular, it is $\dot{V} < 0$, $\forall \dot{\boldsymbol{x}} \ne \boldsymbol{0}$, $\boldsymbol{e} \ne \boldsymbol{0}$, $\dot{\boldsymbol{s}} \ne 0$, while $\dot{V} = 0$ implies $\dot{\boldsymbol{x}} = \boldsymbol{0}$, $\boldsymbol{e} = \boldsymbol{0}$, $\dot{s} = 0$. Note that $\boldsymbol{e} = \boldsymbol{0}$ implies $\Delta \boldsymbol{f} = 0$ through (6)–(8). Hence, the state z is uniformly bounded in Z and local asymptotic stability around $z = (\boldsymbol{0}^T \boldsymbol{0}^T 0)^T$ follows from LaSalle invariant set theorem [16]. Q.E.D.

Remarkably ρ is a free parameter that is not used in the control law (5) and then allows an opportune choice of the feedback gains k_D, k_F, k_I. About the feedback gains, notice that k_P is not involved in the conditions (27), (28) and then is available to meet further design requirements. Also, by increasing k_D, a larger value of Φ can be tolerated. These are considerable improvements over the previous result in [14].

Theorem 1 provides design guidelines to ensure local asymptotic stability of the system (16), (17). A further result can be established to prove local exponential stability.

Theorem 2: There exists a choice of feedback gains k_P, k_D, k_F, k_I that makes the origin of the state space for the system (16), (17) locally exponentially stable. □

Proof: Consider the Lyapunov function candidate

$$W = \frac{1}{2} z^T Q z \tag{30}$$

where

$$Q = \begin{pmatrix} B & -\beta B & -\gamma B n \\ -\beta B & (k_P + \beta k_D) I + k_F' k\, n n^T & (k_I k + \gamma k_D) n \\ -\gamma n^T B & (k_I k + \gamma k_D) n^T & \beta k_I k + \gamma (k_P + k_F' k) \end{pmatrix} \tag{31}$$

with $\beta, \gamma > 0$. Computing the time derivative of W along the trajectories of the system (16), (17) gives

$$\dot{W} = -\dot{x}^T (k_D I - \beta B) \dot{x} - e^T (\beta k_P I + (\beta k_F' k - k_I k - \gamma k_D) n n^T) e - \gamma k_I k s^2 - \gamma \dot{x}^T B n n^T e - (\beta e^T + \gamma s n^T) C^T \dot{x} \tag{32}$$

in which the skew-symmetry of the matrix $\dot{B} - 2C$ has been exploited again.

In view of (14), the function candidate (30), (31) can be lower-bounded as

$$W \geq \frac{1}{2} (\dot{x}^T B \quad e^T) \begin{pmatrix} (1/2\lambda_M) I & -\beta I \\ -\beta I & (k_P + \beta k_D) I \end{pmatrix} \begin{pmatrix} B \dot{x} \\ e \end{pmatrix} + \frac{1}{2} (\dot{x}^T B \quad s n^T) \begin{pmatrix} (1/2\lambda_M) I & -\gamma I \\ -\gamma I & \gamma (k_P + k_F' k) I \end{pmatrix} \begin{pmatrix} B \dot{x} \\ s n \end{pmatrix} + \frac{1}{2} (\dot{s} \quad s) \begin{pmatrix} k_F' k & k_I k + \gamma k_D \\ k_I k + \gamma k_D & \beta k_I k \end{pmatrix} \begin{pmatrix} \dot{s} \\ s \end{pmatrix}. \tag{33}$$

Equation (33) reveals that there exists a choice of k_P, k_D, k_F, k_I, β, and γ that makes W positive definite, provided that:

$$k_P + \beta k_D > 2\beta^2 \lambda_M \tag{34}$$

$$k_P + (1 + k_F) k > 2\gamma \lambda_M \tag{35}$$

$$\beta (1 + k_F) k_I k^2 > (k_I k + \gamma k_D)^2. \tag{36}$$

On the other hand, the function candidate (30), (31), in view of (14) and the inequalities

$$-\dot{x}^T B e \leq \frac{\lambda_M}{2} \left(\frac{\|\dot{x}\|^2}{\eta_1} + \eta_1 \|e\|^2 \right) \qquad \eta_1 > 0 \tag{37}$$

$$-s \dot{x}^T B n \leq \frac{\lambda_M}{2} \left(\frac{\|\dot{x}\|^2}{\eta_2} + \eta_2 s^2 \right) \qquad \eta_2 > 0 \tag{38}$$

$$\dot{s} s \leq \frac{1}{2} \left(\frac{\dot{s}^2}{\eta_3} + \eta_3 s^2 \right) \qquad \eta_3 > 0 \tag{39}$$

can be upper bounded as

$$W \leq H_1 = \frac{1}{2} \left(1 + \frac{\beta}{\eta_1} + \frac{\gamma}{\eta_2} \right) \lambda_M \|\dot{x}\|^2 + \frac{1}{2} (k_P + \beta k_D + \beta \eta_1 \lambda_M) \|e\|^2 + \frac{1}{2} (\beta k_I k + \gamma (k_P + k_F' k) + \eta_3 (k_I k + \gamma k_D) + \gamma \eta_2 \lambda_M) s^2 + \frac{1}{2} \left(k_F' k + \frac{1}{\eta_3} (k_I k + \gamma k_D) \right) \dot{s}^2. \tag{40}$$

Consider the region of the state space

$$Z' = \{z : \|z\| < \Theta\}. \tag{41}$$

The last term in (32) can be upper bounded in the region (41) as

$$-(\beta e^T + \gamma s n^T) C^T \dot{x} \leq (\beta + \gamma) \Theta k_C \|\dot{x}\|^2. \tag{42}$$

In view of (14) and the inequality

$$-\dot{x}^T B\, n n^T e \leq \frac{\lambda_M}{2} \left(\frac{\|\dot{x}\|^2}{\eta_4} + \eta_4 \|e\|^2 \right) \qquad \eta_4 > 0 \tag{43}$$

the function (32) can be upper bounded as

$$\dot{W} \leq -H_2 = -\left(k_D - \beta \lambda_M - \gamma \frac{\lambda_M}{2\eta_4} - (\beta + \gamma) \Theta k_C \right) \|\dot{x}\|^2 - \left(\beta k_P - \gamma \frac{\eta_4 \lambda_M}{2} \right) \|e\|^2 - \gamma k_I k s^2 - (\beta k_F' k - k_I k - \gamma k_D) \dot{s}^2. \tag{44}$$

By comparison of (44) with (40), it can be recognized that if the following inequalities are satisfied for some $\alpha > 0$,

$$k_D - \beta \lambda_M - \gamma \frac{\lambda_M}{2\eta_4} - (\beta + \gamma) \Theta k_C \geq \frac{\alpha}{2} \left(1 + \frac{\beta}{\eta_1} + \frac{\gamma}{\eta_2} \right) \lambda_M \tag{45}$$

$$\beta k_P - \gamma \frac{\eta_4 \lambda_M}{2} \geq \frac{\alpha}{2} (k_P + \beta k_D + \beta \eta_1 \lambda_M) \tag{46}$$

$$\gamma k_I k \geq \frac{\alpha}{2} (\beta k_I k + \gamma (k_P + (1 + k_F) k) + \eta_3 (k_I k + \gamma k_D) + \gamma \eta_2 \lambda_M) \tag{47}$$

$$\beta (1 + k_F) k - k_I k - \gamma k_D \geq \frac{\alpha}{2} \left((1 + k_F) k + \frac{1}{\eta_3} (k_I k + \gamma k_D) \right) \tag{48}$$

the chain of inequalities holds

$$\dot{W} \leq -H_2 \leq -\alpha H_1 \leq -\alpha W \tag{49}$$

and then

$$W(t) \leq W(0) \exp(-\alpha t). \tag{50}$$

For a given Θ, it is possible to choose the gains k_P, k_D, k_F, k_I and the parameters β, γ, η_1, η_2, η_3, η_4 so that the relations (34)–(36) and (45)–(48) are satisfied for some $\alpha > 0$. By virtue of (50), local exponential stability of the system (16), (17) at the origin of the state space is obtained. Further, α allows the computation of a lower bound on the convergence rate toward the equilibrium state. Q.E.D.

About the feedback gains, notice that now k_P is involved in the conditions (34), (35), (46), (47). By means of the free parameters β, γ, η_1, η_2, η_3, η_4, which are not used in the control law (5), however, it is possible to find a set of feedback gains k_P, k_D, k_F, k_I that guarantee local exponential stability.

V. Case Study

The proposed force/position controller was tested in a case study on the six-joint industrial robot COMAU SMART 6.10R. This is an elbow manipulator geometry with zero shoulder offsets and spherical wrist; only the first three joints were considered. The complete numerical data for the robot parameters can be found in [23]. Simulations were run in MATLAB on a PC-486/33.

A step motion from $x = (1.100\ 0\ 0)^T$ $[m]$ to the set point $x_d = (1.120\ 0\ 0)^T$ $[m]$ was commanded to the manipulator's tip. The set point $f_d = 0$ was assigned for the tip force. The geometry of the contact plane is characterized by $n = (1\ 0\ 0)^T$ and $x_0 = (1.115\ 0\ 0)^T$ $[m]$; different values for the stiffness coefficient k were considered. It can be recognized that an unexpected impact occurs along the normal direction to the plane at a distance of 0.005 $[m]$ from the target point x_d. For simplicity, the time scale in the simulations is reset ($t = 0$) at the instant of the impact; further, the sole x-component of position and force vectors are reported, in view of the particular task geometry.

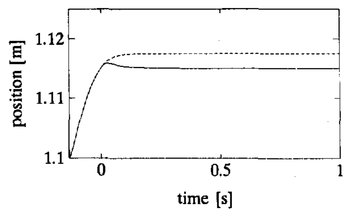

Fig. 2. Time history of the tip position (solid: force/position controller, dashed: position controller).

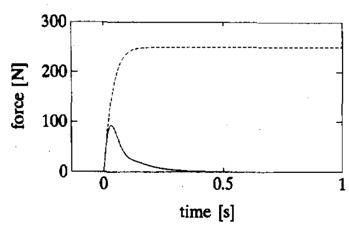

Fig. 3. Time history of the contact force (solid: force/position controller, dashed: position controller).

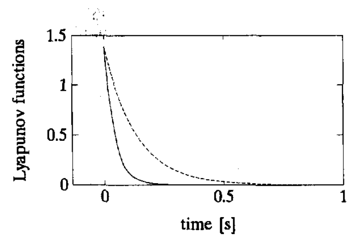

Fig. 4. Time history of the Lyapunov function (30), (31) (solid) and its bounding exponential function (dashed).

The gains in (5) were set to $k_P = 10^5\ [Nm^{-1}]$, $k_D = 10^4\ [Nsm^{-1}]$, $k_F = 4$, $k_I = 55\ [s^{-1}]$. On one hand, k_P and k_D were chosen so as to guarantee a well-damped behavior for the unconstrained motion of the manipulator in a large region of the workspace. On the other hand, k_F and k_I were chosen so as to achieve a satisfactory behavior during the constrained motion with an estimate of the stiffness coefficient of $k = 10^5\ [Nm^{-1}]$. With the above values, the design conditions (27), (28) were satisfied with some $\rho > 0$ for available estimates of λ_M and k_C.

In the following, the numerical results of two simulation runs with a sampling time of 2 $[ms]$ are presented.

In the first run, it is $k = 10^5\ [Nm^{-1}]$. For the purpose of comparison, both the full force/position controller and the pure position controller ($k_F = 0$, $k_I = 0$) were used. It can be seen that the equilibrium position $\boldsymbol{x}_\infty$ ($= \boldsymbol{x}_0$ in this case) is reached (Fig. 2) and the contact force is null at steady state (Fig. 3), so as desired. Notice also that, without force feedback, finite steady-state errors occur both for position and force. Fig. 4 reports the time history of the Lyapunov function $W(t)$ in (30), (31), together with the function $W(0)\exp(-\alpha t)$; the value of α was computed via the MATLAB optimization function CONSTR applied to the set of conditions (34)–(36), (45)–(48) with free parameters β, γ, η_1, η_2, η_3, η_4. It is easy to recognize the exponential stability result established by (50).

In the second run, the robustness of the proposed controller was tested by changing the stiffness coefficient into $k = 10^6\ [Nm^{-1}]$ but leaving the same feedback gains as above. The results of Fig. 5 and Fig. 6 demonstrate that satisfactory performance is obtained even when tuning of the force feedback gains was done by underestimating the actual stiffness of the environment.

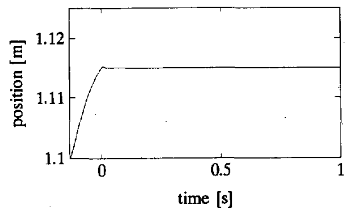

Fig. 5. Time history of the tip position with imprecise stiffness estimate.

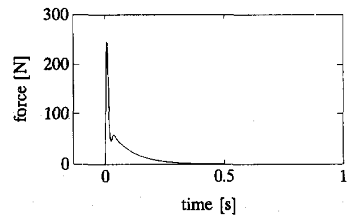

Fig. 6. Time history of the contact force with imprecise stiffness estimate.

VI. Conclusion

Force/position regulation of robot manipulators in contact with an elastically compliant surface was analyzed in this work. The controller consists of a PD action on the position loop, a PI action on the force loop, together with gravity compensation and desired contact force feedforward.

Both local asymptotic stability and exponential stability were proven via the Lyapunov method, thanks to the introduction of off-diagonal terms in the Lyapunov functions. In particular, those terms feature positive constants that serve as additional degrees of freedom to satisfy conditions on the feedback gains but remarkably are not used by the control law.

A case study was developed for an industrial elbow manipulator, whose tip experiences an unexpected impact with the environment on the way toward the target position. The numerical results of two sets of simulations confirmed the theoretical derivation. Exponential stability was verified and robustness of the scheme to imprecise estimate of contact stiffness was successfully tested.

Current work is devoted to investigate the stability of the scheme in the case of imperfect compensation of the gravity term and possibly resort to an adaptation mechanism on the system state.

References

[1] D. E. Whitney, "Historical perspective and state of the art in robot force control," *Int. J. Robotics Research*, vol. 6, no. 1, pp. 3–14, 1987.

[2] N. Hogan, "Impedance control: An approach to manipulation, Parts I–III," *ASME J. Dynamic Systems, Measurement, & Contr.*, vol. 107, pp. 1–24, 1985.

[3] H. Kazerooni, P. K. Houpt, and T. B. Sheridan, "Robust compliant motion for manipulators," *IEEE J. Robotics & Automation*, vol. 2, pp. 83–105, 1986.

[4] M. H. Raibert and J. J. Craig, "Hybrid position/force control of manipulators, *ASME J. Dynamic Systems, Measurement, & Contr.*, vol. 103, pp. 126–133, 1981.

[5] O. Khatib, "A unified approach for motion and force control of robot manipulators," *IEEE J. Robotics & Automation*, vol. 3, pp. 43–53, 1987.
[6] T. Yoshikawa, "Dynamic hybrid position/force control of robot manipulators—Description of hand constraints and calculation of joint driving force," *IEEE J. Robotics & Automation*, vol. 3, pp. 386–392, 1987.
[7] A. De Luca, C. Manes, and F. Nicolò, "A task space decoupling approach to hybrid control of manipulators," in *Proc. 2nd IFAC Symp. on Robot Control*, Karlsruhe, D, 1988, pp. 157–162.
[8] J. T. Wen and S. Murphy, "Stability analysis of position and force control for robot arms," *IEEE Trans. Automat. Contr.*, vol. 36, pp. 365–371, 1991.
[9] N. H. McClamroch and D. Wang, "Feedback stabilization and tracking of constrained robots," *IEEE Trans. Automat. Contr.*, vol. 33, pp. 419–426, 1988.
[10] J. K. Mills and A. A. Goldenberg, "Force and position control of manipulators during constrained motion tasks," *IEEE Trans. Robotics & Automation*, vol. 5, pp. 30–46, 1989.
[11] S. Chiaverini and L. Sciavicco, "Force/position control of manipulators in task space with dominance in force," in *Proc. 2nd IFAC Symp. Robot Control*, Karlsruhe, D, 1988, pp. 137–143.
[12] S. Chiaverini, "Controllo in forza di manipolatori," Ph.D. dissertation, Dept. Computer & Systems Eng., Università degli Studi di Napoli Federico II, Napoli, Italy, 1990.
[13] S. Chiaverini and L. Sciavicco, "The parallel approach to force/position control of robotic manipulators," *IEEE Trans. Robotics & Automation*, vol. 9, pp. 361–373, 1993.
[14] S. Chiaverini and B. Siciliano, "On the stability of a force/position control scheme for robot manipulators," in *Proc. 3rd IFAC Symp. on Robot Control*, Vienna, A, 1991, pp. 183–188.
[15] S. Arimoto and F. Miyazaki, "Stability and robustness of PID feedback control for robot manipulators of sensory capability," in *Robotics Research: 1st Int. Symp.*, M. Brady and R. P. Paul (Eds.). Boston, MA: MIT Press, 1984, pp. 783–799.
[16] J. P. LaSalle, "Some extensions of Liapunov's second method," *IRE Trans. Circuit Theory*, vol. 7, pp. 520–527, 1960.
[17] J. Lončarić, "Normal forms of stiffness and compliance matrices," *IEEE J. Robotics and Automation*, vol. 3, pp. 567–572, 1987.
[18] M. Takegaki and S. Arimoto, "A new feedback method for dynamic control of manipulators," *ASME J. Dynamic Systems, Measurement, & Contr.*, vol. 103, pp. 119–125, 1981.
[19] D. Koditschek, "Natural motion of robot arms," in *Proc. 23rd IEEE Conf. Decision & Contr.*, Las Vegas, NV, 1984, pp. 733–735.
[20] J.-J. E. Slotine and W. Li, "Adaptive strategies in constrained manipulators," in *Proc. 1987 IEEE Int. Conf. Robotics & Automation*, Raleigh, NC, 1987, pp. 595–601.
[21] P. Tomei, "Adaptive PD controller for robot manipulators," *IEEE Trans. Robotics & Automation*, vol. 7, pp. 565–570, 1991.
[22] R. Ortega and M. W. Spong, "Adaptive motion control of rigid robots: A Tutorial," *Automatica*, vol. 25, pp. 877–888, 1989.
[23] L. Villani, "Analisi di stabilità di un algoritmo di controllo parallelo forza/posizione di manipolatori," (in Italian), Masters' thesis, Dept. Computer & Systems Eng., Università degli Studi di Napoli Federico II, Napoli, Italy, 1992.

Robust Stabilization: Some Extensions of the Gain Margin Maximization Problem

Andrzej W. Olbrot and Marek Nikodem

***Abstract*— We consider robust stabilization for SISO systems with linear dependence on a real uncertain parameter which may occur either in the numerator or denominator of the plant transfer function. We show necessary and sufficient conditions for the existence of robust controllers. Their structure and parameterization can be obtained from the corresponding Nevanlinna–Pick interpolation problems. This work extends the previously known case of an uncertain gain parameter.**

I. Introduction

The problem of reducing consequences of uncertainty has been a central issue in the field of control systems. One of the most important problems in robust control theory is robust stabilization. The general problem of robust stabilization can be formulated as follows: given a model of the plant with uncertain parameters, find a compensator which stabilizes the plant regardless of the values of uncertain parameters. In the most recent works on robust stabilization, emphasis has been placed on the analysis part [1]. On the other hand, very little has been done concerning the synthesis of robust controllers. Few results are known for structured (parametric) uncertainties which give not only necessary and sufficient conditions for the controller to exist, but also particular solutions parameterized in terms of arbitrary holomorphic functions [2]. Some of such problems have been solved using techniques from complex analysis, particularly the Nevanlinna–Pick interpolation procedure [2]–[4] which is also known to be useful in network theory (circuit modeling and passive circuits synthesis [7]. The so-called Nevanlinna recursion provides an easy constructive algorithm yielding the unique solution in the "degenerate case" and a parameterization of all solutions in the "nondegenerate case" [4], [7]. Knowing the plant right-half plane (RHP) poles and zeros, the computations can even be done with pencil and paper. In [2], Tannenbaum considers the problem of stabilizing a parameterized family of plants $P_k(s)$ where k takes the values in some compact set K. This problem, in general, has no solutions (he indicated some counter examples). For certain cases, however, it is possible to give an algorithmic solution. In particular, he solved the case of uncertainty in the gain factor (the gain margin problem) $P_k(s) = kP_0(s)$, where $k \in [a, b]$.

Later, Khargonekar and Tannenbaum [4] described a general methodology for using the Nevanlinna–Pick interpolation in several control problems, and as an example, they considered the case of $P(s) = \tilde{P}(s)/(s-\gamma)$, where $\tilde{P}(s)$ is a fixed real rational function and γ is an uncertain parameter, $\gamma \in [a_0 - \alpha,\ a_0 + \beta]$. In the recent paper [8] this problem has been extended to several uncertain poles which cannot move freely and must lie on a specified curve determined by exactly one uncertain coefficient in the plant's denominator.

In our work we consider the case of one uncertain parameter in the plant transfer function which has the following structure $P(s) = (N(s) + k\tilde{N}(s))/D(s)$ or $P(s) = N(s)/(D(s) + k\tilde{D}(s))$ where $k \in [a, b]$, $k \in R$. This extends the results in [4], [8]. Using the techniques from the interpolation theory, we transform the robust stabilization problems to interpolation problems. Then we give necessary and sufficient conditions for the existence of robust stabilizers.

Manuscript received July 6, 1992; revised February 10, 1993.
The authors are with the Department of Electrical and Computer Engineering, Wayne State University, Detroit, MI 48202.
IEEE Log Number 9216422.

0018–9286/94$04.00